Entanglement of the orbital angular momentum states of the photons generated in a hot atomic ensemble

Qun-Feng Chen, Bao-Sen Shi, Yong-Sheng Zhang, and Guang-Can Guo
Key Laboratory of Quantum Information, University of Science and Technology of China, Hefei, 230026, People's Republic of China
(Dated: February 19, 2013)

Quantum protocols will be more efficient with high-dimensional entangled states. Photons carrying orbital angular momenta can be used to create a high-dimensional entangled state. In this paper we experimentally demonstrate the entanglement of the orbital angular momentum between the Stokes and anti-Stokes photons generated in a hot atomic ensemble using spontaneous four-wave-mixing. This experiment also suggests the existence of the entanglement concerned with spatial degrees of freedom between the hot atomic ensemble and the Stokes photon.

PACS numbers: 42.50.Dv, 32.80.-t, 03.65.Wj, 03.67.Mn

arXiv:0807.0130v1 [quant-ph] 1 Jul 2008

Entanglement is one of the most fantastic phenomenon of quantum mechanics, and is used as a resource in quantum information field[1]. High-dimensional two-particle entangled states can be used to realize some quantum information protocols more efficiently [2, 3]. Photons carrying orbital angular momenta (OAM) are used to create high-dimensional entangled states, since OAM can be used to define an infinite-dimensional Hilbert space [4]. The first experiment of the entanglement of the OAM states generated via spontaneous parametric down-conversion in a nonlinear crystal was demonstrated in 2001[5], since then several protocols based on OAM states of photons have been realized experimentally[6, 7, 8]. The transferring of OAM between classical light and cold atoms[9, 10, 11] and hot atoms[12] has also been reported in the past years. Recently, the entanglement of OAM states of the photons generated in a cold atomic system using Duan-Lukin-Cirac-Zoller (DLCZ) scheme[13] has been clarified by Inoue *et al.*[14]. So far, there is no experimental discussion about the entanglement of the OAM states of the photons generated in a hot atomic system. In this paper we demonstrate the entanglement of OAM states of the photons generated in a hot atomic ensemble using the spontaneous four-wave-mixing (SFWM)[15, 16]. Our experiment is different from the experiment done by Inoue *et al.*: In our experiment, SFWM is used to generate a photon pair, in contrast with the experiment of Ref. [14], in which the method based on DLCZ scheme is used. Furthermore, our experiment is based on a hot atomic ensemble, which is more easy to be realized compared with the scheme based on a cold atomci system. In our experiment, we clearly demonstrate the entanglement of the OAM between the Stokes and anti-Stokes photons generated via SFWM in a hot atomic ensemble, the concurrence got in this experiment is about 0.81. This experiment also suggests the existence of the entanglement concerned with spatial degrees of freedom between the hot atomic ensemble and the Stokes photon.

The schematic setup used in this experiment is shown in Fig. 1. The energy levels and the frequencies of the lasers used are shown in Fig. 1(a). A strong coupling laser, which is resonant with the $|b\rangle \rightarrow |c\rangle$ transition, drives the populations of the atoms into level $|a\rangle$. A weak pump laser, resonant with the $|a\rangle \rightarrow |d\rangle$ transition, is applied to the system. The $|d\rangle \rightarrow |b\rangle$ transition will be induced by the pump laser and the Stokes (S) photons will be generated. When a Stokes photon is emitted, the atomic ensemble collapses into the state $\frac{1}{\sqrt{N}}\sum_j |a_1, a_2, \ldots, b_j, \ldots, a_N\rangle$. The strong coupling laser repumps the atomic ensemble back to the state $|a_1, a_2, \ldots a_N\rangle$, and an anti-Stokes (AS) photon is generated. In this process, the energy, momentum and OAM of the photons will be conserved[12, 17],i. e.,

$$\begin{aligned} \omega_{\rm S} + \omega_{\rm AS} &= \omega_{\rm P} + \omega_{\rm C}, \\ \vec{k}_{\rm S} + \vec{k}_{\rm AS} &= \vec{k}_{\rm P} + \vec{k}_{\rm C}, \\ L_{\rm S} + L_{\rm AS} &= L_{\rm P} + L_{\rm C}\,, \end{aligned} \tag{1}$$

where the ω_i, $\vec{k}_i$ and L_i represent the frequency, wave vector and OAM of the corresponding photons respectively. According to Eq. (1), when the pump and coupling lasers carry zero OAM, the Stokes and anti-Stokes photons will be in the entangled state of

$$|\Psi\rangle = C \sum_{i=-\infty}^{+\infty} \alpha_i |i\rangle_{\rm S} |-i\rangle_{\rm AS}\,, \tag{2}$$

where C is the normalization coefficient, α_i are the relative amplitudes of the OAM states. In this work we only investigate the entanglement concerned with $i = 0$ and 1, thus the experimental expected entangled state can be written as:

$$|\Psi\rangle = C(|0\rangle_{\rm S}|0\rangle_{\rm AS} + \alpha_1 |1\rangle_{\rm S}|-1\rangle_{\rm AS})\,. \tag{3}$$

Although we only discuss the two dimensional case, it is natural to presume that our discussion can be extended into high-dimensional cases over a wide range of OAM[14].

A Gaussian mode beam carrying the well-defined OAM is in Laguerre-Gaussian (LG) mode[18], it can be described by LG_{pl} mode, where $p+1$ is the number of the

radial nodes, and l is the number of the 2π-phase variations along a closed path around the beam center. Here we only consider the cases of $p = 0$. The LG_{0l} mode carries the corresponding OAM of $l\hbar$ per photon and has a doughnut-shape intensity distribution:

$$E_{0l}(r,\varphi) = E_{00}(r)\frac{1}{\sqrt{|l|!}}\left(\frac{r\sqrt{2}}{w}\right)^{|l|} e^{-il\varphi}, \qquad (4)$$

where

$$E_{00}(r) = \sqrt{\frac{2}{\pi}}\frac{1}{w}\exp\left(-\frac{r^2}{w^2}\right)$$

is the intensity distribution of a Gaussian mode beam which carries zero OAM (LG_{00}) and w is the beam waist. In most cases, computer-generated holograms (CGH) are used to create the LG modes of various orders[19]. The superposition of the LG_{00} mode and the LG_{01} mode can be achieved by shifting the dislocation of the hologram out of the beam center a certain amount[5, 20].

In this paper, a CGH combined with a single-mode fiber are used for mode discrimination. The ±1 order diffraction of the CGH increases the OAM of the input beam by $\pm1\hbar$ per photon when the dislocation of the hologram is overlapped with the beam center. The first order diffraction of the CGH is coupled into the single-mode fiber. The single-mode fiber collects only the Gaussian mode beam, therefore the combination of the CGH and the single-mode fiber can be used to select the $LG_{0\mp1}$ or LG_{00} mode or the superposition of the them, according to which of the ±1 order diffraction of the hologram is coupled and the displacement of the hologram. It should be noted that there are also higher order LG modes in the first order diffraction, but they are very small compared with the $LG_{0\pm1}$ mode[20] and the influence of them is ignored in this paper.

The schematic experimental setup is shown in Fig. 1(b). A natural rubidium cell with a length of 5 cm is used as the working medium. The temperature of the cell is kept at about 50°C, corresponding to an atomic intensity of about $1 \times 10^{11}/\text{cm}^3$. The coupling laser, which is vertically linear polarized, is resonant with the $|5S_{1/2}, F = 2\rangle \rightarrow |5P_{1/2}, F = 2\rangle$ transition of ^{87}Rb. The intensity of the coupling laser is about 7 mW. The pump laser, which is counter-propagating with the coupling laser and horizontally polarized, is resonant with the $|5S_{1/2}, F = 1\rangle \rightarrow |5P_{3/2}, F = 2\rangle$ transition of ^{87}Rb. The power of the pump is about 60μW. The $1/e^2$ diameters of these two lasers are about 2 mm. The vertically polarized Stokes photons emitted at an angle of about 4° to the lasers are diffracted by a CGH (H1), and the -1 order diffraction of the H1 is coupled into a single-mode fiber (SMF1) after being filtered by the F1. The diffraction of the H1 decreases the OAM of the input photons by $1\hbar$ when the displacement of H1 is 0. The displacement of the CGH is defined as the distance between the dislocation of the CGH and the beam center. The horizontally

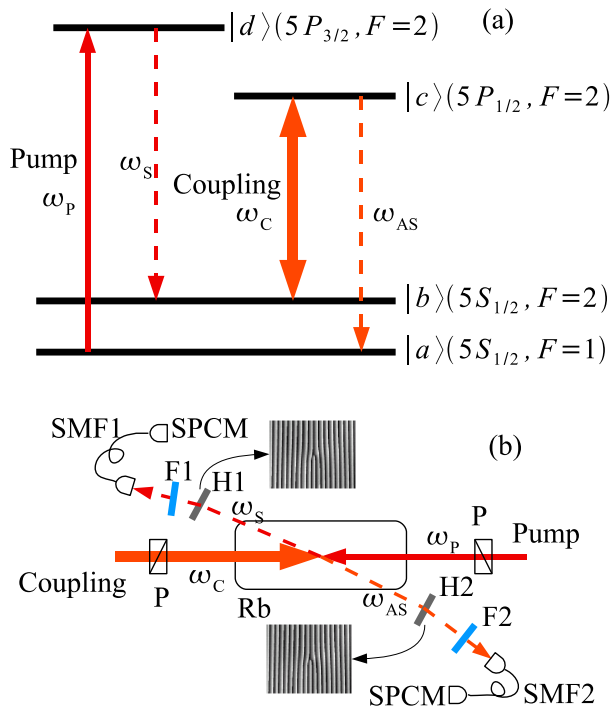

FIG. 1: (Color online) (a) Energy levels and frequencies of the lasers used in this experiment. (b) Schematic setup of our experiment. A strong coupling and a weak pump laser, which are resonant with $|5S_{1/2}, F = 2\rangle \rightarrow |5P_{1/2}, F = 2\rangle$ and $|5S_{1/2}, F = 1\rangle \rightarrow |5P_{3/2}, F = 2\rangle$ transitions of ^{87}Rb respectively, are in counter propagating. Pairs of correlated Stokes and anti-Stokes photons are generated in phase-matched directions. H1 and H2 are computer-generated holograms; SMF1 and SMF2 are single-mode fibers, which are connected to single photon counting modules(SPCM); F1 and F2 are filters.

polarized anti-Stokes photons in the phase matched direction are diffracted by the other CGH (H2). The +1 order diffraction is coupled into SMF2 after being filtered by F2, which increases the OAM of the collected anti-Stokes photons by $1\hbar$ at 0 displacement. The diffraction efficiency of the CGHs used in this experiment are about 40%. Each of the filters F1 and F2 consists of an optical pumped paraffin-coated ^{87}Rb cell and a ruled diffraction grating. The optical pumped rubidium cell is used to filter out the scattering of the co-propagating laser, and the ruled diffraction grating is used to separate the photons at the D1 and D2 transitions. The collected photons are detected by photon-counting modules (Perkin-Elmer SPCM-AQR-15). The time resolved coincident statistics of the Stokes and anti-Stokes photons are accumulated by a time digitizer (FAST ComTec P7888-1E) with 2 ns bin width and totally 160 bins. In this experiment the Stokes photons are used as the START of the P7888-1E and the anti-Stokes photons after certain delay are used as the STOP of the P7888-1E.

The time resolved coincident counts of the Stokes and

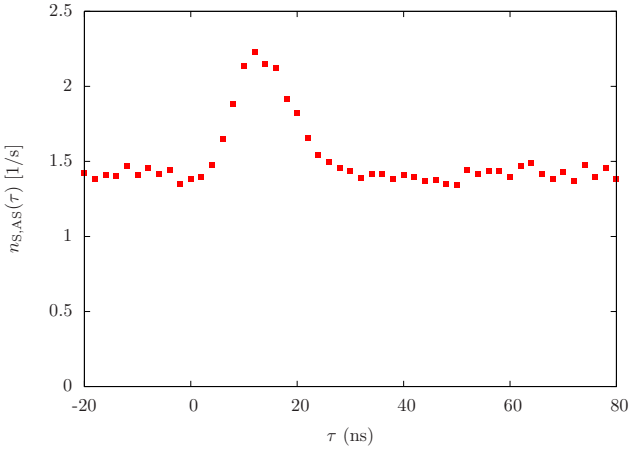

FIG. 2: (Color online) Time resolved coincidence counting between the Stokes and anti-Stokes photons. The data is accumulated about 1000 seconds and then normalized in time. τ is the relative delay between the Stokes and anti-Stokes photons. The delay between the Stokes photons and anti-Stokes photons is cause by time used to generate anti-Stokes photons, which is mainly determined by the Rabi frequency of coupling field[15].

anti-Stokes photons when the displacement of the both CGHs are far larger than the waists of the beam are shown in Fig. 2. When the displacement of a CGH is far larger than the waist of a beam, the CGH almost does not affect the mode of the photons, therefore Fig. 2 shows the coincidence between the Stokes and anti-Stokes photons in LG_{00} mode. The maximum coincident counts are obtained at the relative delay of 12 ns between the Stokes and anti-Stokes photons, which gives a correlation function of $g_{S,AS}(12\text{ ns}) = 1.57 \pm 0.04$. The counting rates of the Stokes and anti-Stokes photons are 1.4×10^4/s and 4.0×10^4/s respectively. The larger counting rates of the anti-Stokes photons is caused by the atoms moving out and in the coupling beam quickly, which makes a large effective decay rate between the ground states. The atoms in the state $|b\rangle$ moving into the coupling laser contribute to uncorrelated anti-Stokes photons. Even when the pump beam is absent the counting rate of the anti-Stokes is larger than 20000/s. These uncorrelated counts causes the large background in the coincidence between the Stokes and anti-Stokes photons, as shown in Fig. 2. From Fig. 2 we found that the correlated time between the Stokes and anti-Stokes photons is less than 30 ns.

In order to evaluate the quantum correlation of the OAM states, we measure the coincident counts with various displacements of the holograms. Figure 3 shows the results when the H1 is fixed at various displacement while the displacement of H2 is swept. Every point is got by $N = \sum_{\tau=2\text{ns}}^{32\text{ns}}(N(\tau) - bg)/bg$, where $N(\tau)$ is the counting rate of each bin and bg is background counting rate which is got by averaging the coincidences between the Stokes and anti-Stokes photons when $\tau > 50$ ns. This guarantees that most of the correlated anti-Stokes photons are taken into account. Every point is accumulated over 500 seconds. The data are fitted with the square of the projection function[19]:

$$a(x0) = \iint e^{-i\arg(r\cos\varphi - x0, r\sin\varphi)} \times u_{AS}(r) u_S(r,\varphi)^* r\,\mathrm{d}r\,\mathrm{d}\varphi\,, \quad (5)$$

where $\arg(x,y)$ is the argument of the complex number $x+i\,y$, $e^{-i\arg(r\cos\varphi - x0, r\sin\varphi)}$ represents the transmitting function of H2 with displacement of $x0$, $u_{AS}(r) = E_{00}(r)$ is the field amplitude of the anti-Stokes photons collected by the single-mode fiber after being diffracted by the hologram, and $u_S(r,\varphi) = \cos\theta E_{00}(r) + \sin\theta E_{01}(r,\varphi)$ is the field amplitude of the Stokes photons collected by the single-mode fiber. The superposition of the LG_{00} and LG_{01} modes can be controlled by the displacement of H1. Equation (5) gives the projection between the different OAM modes. In this paper the u_is are the amplitudes of the Stokes and anti-Stokes photons respectively. This equation is tenable only when the collapse of the Stokes photons lead the anti-Stokes photons collapse into the corresponding states. Therefore if Eq. (5) always holds no matter the Stokes photons are collapsed to stationary states or superposition states, the Stokes photon and anti-Stokes photon should be in a quantum correlated state. In Fig. 3 (a), the red squares show the results of the coincident counts versus the displacement of H2 when the displacement of H1 is far larger than the waist of the Stokes photons, and the green dots show the results when the displacement of H1 is 0. The red line in Fig. 3 (a) is fitted with $\theta = 0$ and the green dashed line is fitted with $\theta = \pi/2$, which means the Stokes photons are in LG_{00} and LG_{01} modes respectively. This figure demonstrates the collapse of the Stokes photon state into the stationary states lead the anti-Stokes photon state collapse into the corresponding stationary states. Therefore this figure indicates clearly the correlation of OAM between the Stokes and anti-Stokes photons. However, such a correlation can be obtained even in the mixture $|0\rangle_S|0\rangle_{AS}$ and $|1\rangle_S|1\rangle_{AS}$ states. To further demonstrate that the Stokes and anti-Stokes photons are in a quantum correlated state, we displace the H1 with a certain amount, which make the collected Stokes photons be in the superposition states $1/\sqrt{2}(|0\rangle \pm |1\rangle)$, and then sweep H2. The results are shown in Fig. 3 (b). The data fit well with the theoretical prediction, which demonstrates that the anti-Stokes photon state collapses into the corresponding superposition states when the Stokes photon state collapses into the superposition states. Therefore the results shown in Fig. 3 demonstrate that the Stokes and anti-Stokes photons are in strongly quantum correlated OAM states.

To further demonstrate the entanglement of the Stokes and anti-Stokes photons, we perform a two-qubit state tomography[21], and get the full state of the Stokes and anti-Stokes photons. The density matrix is reconstructed from the experimentally obtained coincidences

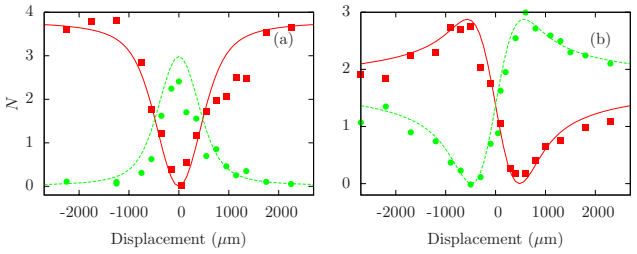

FIG. 3: (Color online) Coincident counts versus the displacement of H2 with different displacement of H1. (a) shows the results that the Stokes photons are in stationary states $|0\rangle$ (red squares) and $|1\rangle$ (green dots); (b) shows the results that the Stokes photons are in the superposition states $(|0\rangle \pm |1\rangle)/\sqrt{2}$. The data are fitted using the square of Eq. (5) with $w = 0.8$ mm.

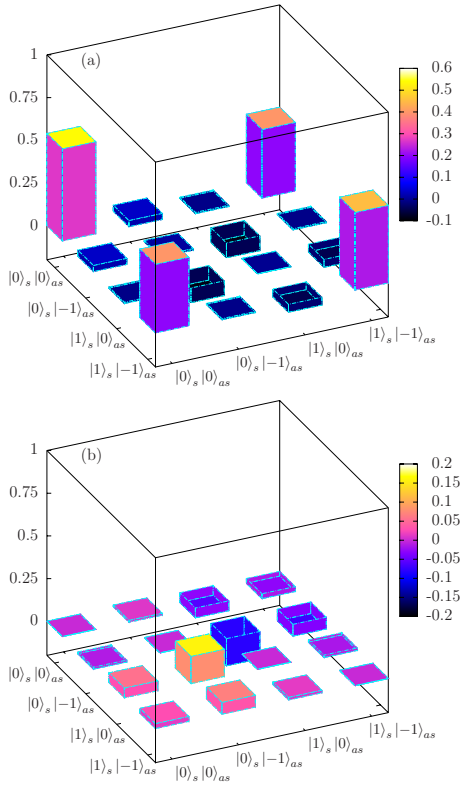

FIG. 4: (Color online) Graphical representation of the reconstructed density matrix. (a) is the real part and (b) is the imaginary part.

with various combinations of the measurement basis. A graphical representation of the reconstructed density matrix is shown in Fig. 4. From the density matrix, the fidelity[22] to the maximally entangled state $|\Psi\rangle = (|0\rangle_S|0\rangle_{AS} + |1\rangle_S|-1\rangle_{AS})/\sqrt{2}$ is estimated to about $\langle\Psi|\rho|\Psi\rangle = 0.89$. The concurrence[23] estimated from the density matrix is about $0.81 > 0$, which demonstrated the Stokes and anti-Stokes photons are in an entangled state clearly[23]. The entanglement of formation[22] is also estimated to be 0.74.

The Stokes photons and the anti-Stokes photons are not generated simultaneously in the SFWM. The atomic ensemble collapses into the state $\frac{1}{\sqrt{N}}\sum_j |a_1, a_2, \ldots, b_j, \ldots, a_N\rangle$ after emitting an Stokes photon, the information of the Stokes photons will be stored in the atomic system firstly. Lately the information of the atomic ensemble is retrieved by the coupling laser, and an anti-Stokes photon is generated[14, 17], the anti-Stokes photon carries the information of the atomic ensemble. The speed of the anti-Stokes photon generated is mainly determined by the Rabi frequency of the coupling laser[15]. Therefore the entanglement of OAM between Stokes photons and the anti-Stokes photons might suggest the existence of the entanglement of OAM between the Stokes photon and the atomic ensemble. Our work is different from the work of V. Boyer *el al.*[24]. In their work they used a four-wave-mixing process[25] to generate the spatially multimode quantum-correlated twin beams with finite OAM in a hot atomic vapor. Their experiment is not a spontaneous process, and is not in the photon level. They also have not demonstrated the entanglement between the beams.

We estimate that the main sources of the errors in this experiment are from follows: the decay rate of the atoms is very large, which causes the large background counting; the instability of the frequency of the lasers; there are also other LG modes in the diffraction except for the LG_{00}, LG_{01} modes and their superposition[19, 20]; the superposition of the state LG_{00} and LG_{01} is got by shifting the hologram, which is dependent on the beam waist, therefore the small fluctuation of the beam position also causes the error.

In summary, we have demonstrated the entanglement of OAM states between the Stokes and anti-Stokes photons generated via SFWM in a hot rubidium cell. The entanglement of the Stokes and anti-Stokes photons also suggests that the Stokes photon might entangle with the hot atomic ensemble in spatial degrees of freedom (OAM in this paper).

Acknowledgments

We thank Pei Zhang for supplying computer-generated holograms and some useful discussion. We also thank Xi-Feng Ren for some useful discussion. This work is supported by National Fundamental Research Program(2006CB921907), National Natural Science Foundation of China(60621064, 10674126, 10674127), the Innovation funds from Chinese Academy of Sciences, and the Program for NCET.

[1] A. Galindo and M. A. Martín-Delgado, Rev. Mod. Phys. **74**, 347 (2002).

[2] M. Bourennane, A. Karlsson, and G. Björk, Phys. Rev. A **64**, 012306 (2001).

[3] H. Bechmann-Pasquinucci and A. Peres, Phys. Rev. Lett. **85**, 3313 (2000).

[4] G. F. Calvo, A. Picon, and E. Bagan, Phys. Rev. A **73**, 013805 (2006).

[5] A. Mair, A. Vaziri, G. Weihs, and A. Zeilinger, Nature **412**, 313 (2001).

[6] A. Vaziri, G. Weihs, and A. Zeilinger, Phys. Rev. Lett. **89**, 240401 (2002).

[7] A. Vaziri, J. W. Pan, T. Jennewein, G. Weihs, and A. Zeilinger, Phys. Rev. Lett. **91**, 227902 (2003).

[8] N. K. Langford, R. B. Dalton, M. D. Harvey, J. L. O'Brien, G. J. Pryde, A. Gilchrist, S. D. Bartlett, and A. G. White, Phys. Rev. Lett. **93**, 053601 (2004).

[9] J. W. R. Tabosa and D. V. Petrov, Phys. Rev. Lett. **83**, 4967 (1999).

[10] S. Barreiro and J. W. R. Tabosa, Phys. Rev. Lett. **90**, 133001 (2003).

[11] S. Barreiro, J. W. R. Tabosa, J. P. Torres, Y. Deyanova, and L. Torner, Opt. Lett. **29**, 1515 (2004).

[12] W. Jiang, Q.-F. Chen, Y.-S. Zhang, and G.-C. Guo, Phys. Rev. A **74**, 043811 (2006).

[13] L. M. Duan, M. D. Lukin, J. I. Cirac, and P. Zoller, Nature **414**, 413 (2001).

[14] R. Inoue, N. Kanai, T. Yonehara, Y. Miyamoto, M. Koashi, and M. Kozuma, Phys. Rev. A **74**, 053809 (2006).

[15] V. Balić, D. A. Braje, P. Kolchin, G. Y. Yin, and S. E. Harris, Phys. Rev. Lett. **94**, 183601 (2005).

[16] Q.-F. Chen, B.-S. Shi, M. Feng, Y.-S. Zhang, and G.-C. Guo, *Generation of nonclassical photon pairs in hot rubidium vapor*, submitted.

[17] M. O. Scully, E. S. Fry, C. H. R. Ooi, and K. Wodkiewicz, Phys. Rev. Lett. **96**, 010501 (2006).

[18] L. Allen, M. W. Beijersbergen, R. J. C. Spreeuw, and J. P. Woerdman, Phys. Rev. A **45**, 8185 (1992).

[19] J. Arlt, K. Dholakia, L. Allen, and M. J. Padgett, J. Mod. Opt. **45**, 1231 (1998).

[20] A. Vaziri, G. Weihs, and A. Zeilinger, J. Opt. B: Quantum Semiclass. Opt. **4**, S47 (2002).

[21] D. F. V. James, P. G. Kwiat, W. J. Munro, and A. G. White, Phys. Rev. A **64**, 052312 (2001).

[22] M. A. Nielsen and I. L. Chuang, *Quantum Computation and Quantum Information* (Cambridge University Press, Cambridge, England, 2000).

[23] W. K. Wootters, Phys. Rev. Lett. **80**, 2245 (1998).

[24] V. Boyer, A. M. Marino, and P. D. Lett, Phys. Rev. Lett. **100**, 143601 (2008).

[25] V. Boyer, C. F. McCormick, E. Arimondo, and P. D. Lett, Phys. Rev. Lett. **99**, 143601 (2007).